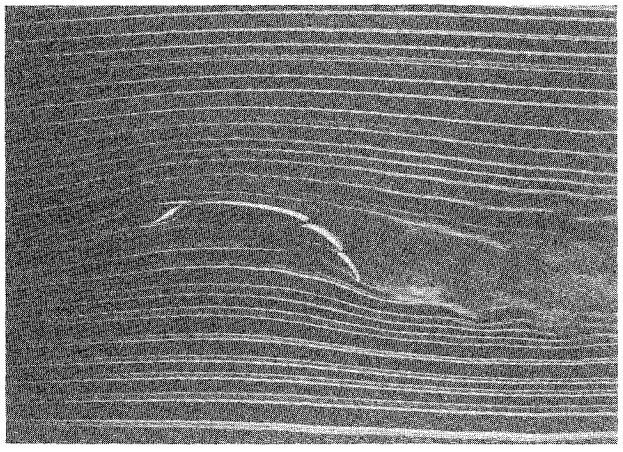

Fig. 3 Visualization of the two-dimensional flow over a four-element airfoil (geometry is same as in Fig.1, $Re_L \approx 0.3 \times 10^6$).

well within the attached flow regions with experimental results,[6] only a limited local validation of the three-dimensional computation was attempted. The large change in the shape of the pressures near the leading edge, along with an effort to simplify the test, influenced the decision to measure the pressures only in this area. The results of these experiments (at $Re_L \approx 0.7 \times 10^6$) with the $\mathcal{R} = 1.5$ wing are shown in Fig. 2 by the rectangular symbols, and they compare well with the computations. The calculated section lift coefficient for the two-dimensional case was $C_L = 3.73$ and for the three-dimensional case $C_L = 1.78$. Because of this large difference, an attempt to follow lift-line practice and to show an "equivalent section angle of attack" (of $C_L = 1.78$) will lead to an extremely large negative incidence.

Experimental attempt to develop such high-lift airfoil shapes in two dimensions becomes difficult, too, because of the high-pressure gradients, shown in Fig. 1. Two-dimensional smoke-trace flow visualization (in Fig. 3) demonstrate this, and a large stalled area is visible behind the main wing. In this particular case, in spite of the large suction peak at the leading edge, the flow is attached there and separates later behind the main wing element. At this low Reynolds number, the boundary layer in the gap between the main wing and the second flap was thick and reduced the momentum transfer to the wing's suction side, resulting in the visible flow separation pattern. However, three-dimensional low visualizations with tufts indicated that for Reynold number of 0.5×10^6 to 2.0×10^6 (based on wing's chord), the $\mathcal{R} = 1.5$ wing had a completely attached flowfield. Further experiments with these wings ($\mathcal{R} = 1.5$) showed that with additional airfoil shape modifications, trailing-edge deflection of up to 90 deg were possible without flow separations (this was equivalent to about $C_L = 4.15$ for the two-dimensional).

Concluding Remarks

This short example shows that highly cambered airfoil shapes cannot be developed, neither experimentally nor numerically, with two dimensional tools. The strong dependency of airfoil shape on the $\mathcal{R}$ requires the definition of wing planform shape first, and only then and only with three-dimensional tools can the airfoil shape be formed (and optimized).

Consequently, experimental development of such wings is extremely difficult and requires an elaborative fabrication procedure. Therefore, even a simplified three-dimensional computational method, such as the one used here, can accelerate a similar multi-element-wing development program.

For high-lift wings with $\mathcal{R}$ and Reynolds number similar to the values mentioned here, trailing-edge flap detection of up to 90 deg is possible without causing flow separations.

Acknowledgments

This work was partially supported by NASA Ames Research Center under Grant No. NCC-2-458, with Dr. Larry Olson as project monitor. The author also acknowledges the technical support provided by Mr. Robert N. Walters during the experimental validation of the computational method.

References

[1]Robinson A. and Laurman, J. A., *Wing Theory*, Cambridge Univ. Press, Cambridge of England, 1956, Chap. 3.

[2]Abbott, I. H. and von Doenhoff, A. E., *Theory of Wing Sections*, Dover, New York, 1959.

[3]Smith, A. M. O., "High Lift Aerodynamics," *Journal of Aircraft*, Vol. 12, 1975.

[4]Nichols, J. H., Jr., and Taylor, D. W., "Development of High Lift Devices for Application to Advanced Navy Aircraft," *Proceedings of the V/STOL Aircraft Aerodynamics Conference*, Monterey, CA, Vol. 2, May 1979, pp.777-849.

[5]Maskew, B., "Program VSAERO," A Computer Program for Calculating the Nonlinear Aerodynamic Characteristics of Arbitrary Configurations," NASA CR-166476, Nov. 1982.

[6]Katz, J., "Evaluation of an Aerodynamic-Load Prediction Method on a STOL Fighter Configuration," AIAA Paper 86-0590, Jan. 1986.

Diffuser Performance of Two-Stream Supersonic Wind Tunnels

Dimitri Papamoschou*
California Institute of Technology, Pasadena, California

Introduction

A SIMPLE theoretical model is presented that determines the inviscid, steady-state diffuser performance of a tunnel with two plane, parallel supersonic streams that come into contact downstream of a splitter plate and form an infinitely thin interface. The model predictions can be useful to the design and operation of two-stream supersonic wind tunnels and of aircraft engines in which mixing is done at supersonic speeds.

A typical one-stream supersonic wind tunnel consists of a converging-diverging nozzle with a given sonic throat area, a test section in which uniform conditions are maintained, and a diffuser with a second throat for decelerating the flow and recovering the pressure. Choking criteria for such wind tunnels determine the minimum allowable second throat area for which the upstream conditions remain unchanged and are well established: assuming perfect-gas law and neglecting viscous effects, the minimum second throat area under steady-state conditions is the sonic throat area of the supersonic nozzle. In that case, pressure recovery is complete because the Mach number at the second throat is sonic and shock wave losses are eliminated.

For a stream with nonuniform distributions of Mach number and gas composition, choking criteria are more complex. The parameter that describes the pressure area relation for uniform or nonuniform flows is

$$\beta = \frac{\partial A}{\partial p} \tag{1}$$

Received Aug. 24, 1988; revision received Sept. 29, 1988.

*Research Fellow, Graduate Aeronautical Laboratories; currently, Assistant Professor, Mechanical Engineering Department, University of California, Irvine. Member AIAA.

as set forth by Ferri and Edelman.[1] This parameter is very useful because it links the pressure area behavior of nonuniform flows with that of uniform flows: a nonuniform flow with a given β behaves as a uniform flow with the same β. For $\beta>0$, the flow acts subsonic; for $\beta<0$, the flow acts supersonic; and, for $\beta=0$, the flow is choked. The latter is the generalized choking criterion.

For inviscid, perfect-gas flow,

$$\beta=\frac{\partial A}{\partial p}=-\frac{1}{\gamma}\frac{A}{p}\frac{M^2-1}{M^2} \tag{2}$$

where A is the stream tube area, p the static pressure, M the Mach number, and γ the specific heat ratio. A nonuniform flow can be approximated by a series of steam tubes with uniform conditions in each. Assuming uniform static pressure across the streamtubes, β is computed as follows:

$$\beta=-\frac{1}{p}\sum_{j=1}^{n}\frac{A_j}{\gamma_j}\frac{M_j^2-1}{M_j^2} \tag{3}$$

where n is the total number of stream tubes in an area

$$A=\sum_{j=1}^{n}A_j$$

The usefulness of β has been demonstrated in the Bernstein et al.[2] analysis of multistream nozzle flow. There, it is shown that the flow chokes at the nozzle throat ($\beta=0$), but the individual stream Mach numbers do not have to be 1. This is in accord with Eq. (3). Additionally, it is shown that, when choking occurs, a weak pressure wave does not propagate upstream, although some individual streams are subsonic. Their findings are in agreement with results presented in this Note, although they did not address the problem of diffuser performance examined here.

Consider now a flow made of two parallel streams with different Mach numbers, equal or unequal specific heat ratios, and uniform pressure across. Assume that the interface between the two streams is infinitely thin. The choking condition is obtained by setting $\beta=0$ in Eq. (3) with $n=2$:

$$\frac{A_1}{\gamma_1}\frac{M_1^2-1}{M_1^2}+\frac{A_2}{\gamma_2}\frac{M_2^2-1}{M_2^2}=0 \tag{4}$$

Equation (4) has been employed in the past for predicting choking in an experimental apparatus where a shear layer was formed between a supersonic and a subsonic stream.[3]

This report examines the consequences of criterion Eq. (4) on the design and operation of two-stream supersonic wind tunnels. Specifically, the following questions are explored: given the test section conditions, what is the process by which the flow reaches the state defined by Eq. (4)? What is the minimum permissible second throat area? And what is the best possible pressure recovery?

Flow Model

In the following model, it is assumed that the flow is inviscid and isentropic, with perfect-gas behavior. We examine the two-dimensional flow geometry depicted in Fig. 1. Two converging-diverging nozzles of sonic-throat areas $A_{1,*}$, and $A_{2,*}$ and exit areas $A_{1,\infty}$ and $A_{2,\infty}$ produce two parallel supersonic streams with test section Mach numbers $M_{1,\infty}$ and $M_{2,\infty}$. The two streams come into contact downstream of a splitter plate and form an infinitely thin interface. At the nozzle exits, the static pressures of the two gases are equal.

Downstream of the constant-area test section starts the diffuser in which the channel area changes slowly enough that the flow can be approximated as one-dimensional. The diffuser walls are shaped such that the static pressures at each side of the interface, p_1 and p_2, are equal at every location along the interface. Thus, the interface remains straight as the conditions change with downstream distance. Since the flow is isentropic, the total pressures of the two streams, p_{t_1} and p_{t_2}, are invariant. This together with the requirement that $p_1=p_2=p$, allows us to establish relations between the diffuser Mach numbers, M_1 and M_2, and the static pressure p. For convenience, we correlate with the normalized pressure

$$\bar{p}=p/p_{t_1}$$

The following expressions for the Mach numbers are obtained by inverting the well-known isentropic formula for total pressure:

$$M_1^2=\frac{2}{\gamma_1-1}\left[\bar{p}^{-(\gamma_1-1)/\gamma_1}-1\right] \tag{5}$$

$$M_2^2=\frac{2}{\gamma_2-1}\left[\left(\bar{p}\frac{p_{t_1}}{p_{t_2}}\right)^{-(\gamma_2-1)\gamma^2}-1\right] \tag{6}$$

Equations (5) and (6) are obtained from conservation of momentum flux and entropy. The diffuser areas A_1 and A_2 that correspond to M_1 and M_2, respectively, are determined from mass flux conservation, expressed in the form of area-Mach number relation:

$$\frac{A_1}{A_{1,*}}=\frac{1}{M_1}\left[\frac{2}{\gamma_1+1}\left(1+\frac{\gamma_1-1}{2}M_1^2\right)\right]^{(\gamma_1+1)/2(\gamma_1-1)} \tag{7}$$

$$\frac{A_2}{A_{2,*}}=\frac{1}{M_2}\left[\frac{2}{\gamma_2+1}\left(1+\frac{\gamma_2-1}{2}M_2^2\right)\right]^{(\gamma_2+1)/2(\gamma_2-1)} \tag{8}$$

Of interest now is how the entire diffuser area $A=A_1+A_2$ changes with $\bar{p}$. It is instructive to normalize A by the combined nozzle-sonic throat area $A_*=A_{1,*}+A_{2,*}$. Thus, we examine the parameter

$$\frac{A}{A_*}=\frac{A_1+A_2}{A_{1,*}+A_{2,*}}$$

$$=\frac{(A_1/A_{1,*})+(A_2/A_{2,*})(A_{2,*}/A_{1,*})}{1+(A_{2,*}/A_{1,*})} \tag{9}$$

where $A_{2,*}/A_{1,*}$ is related to the test section conditions and to the nozzle exit area ratio via

$$\frac{A_{2,*}}{A_{1,*}}=\frac{A_{2,\infty}}{A_{1,\infty}}\frac{A_{1,\infty}}{A_{1,*}}\frac{A_{2,*}}{A_{2,\infty}} \tag{10}$$

Combined Eqs. (5-10) form a complicated expression for A/A_*, written here symbolically as

$$\frac{A}{A^*}=f\left(\bar{p};M_{1,\infty},M_{2,\infty},\gamma_1,\gamma_2,\frac{A_{2,\infty}}{A_{1,\infty}}\right) \tag{11}$$

Figures 2a-2c depict the relations of A/A_*, M_1, and M_2 with $\bar{p}$ for $\gamma_1=\gamma_2=1.4$, $A_{2,\infty}/A_{1,\infty}=1$, and three combinations of freestream Mach numbers. In Fig. 2a, $M_{1,\infty}=M_{2,\infty}=3$, which is the same as one uniform stream at $M=3$. As $\bar{p}$ increases, the area and Mach number decrease un-

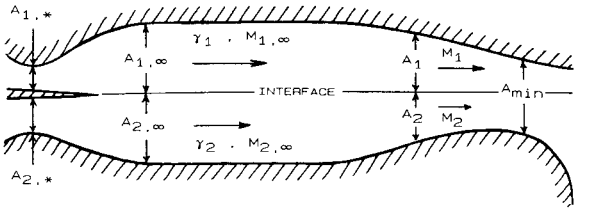

Fig. 1 Flow model geometry and Mach numbers.

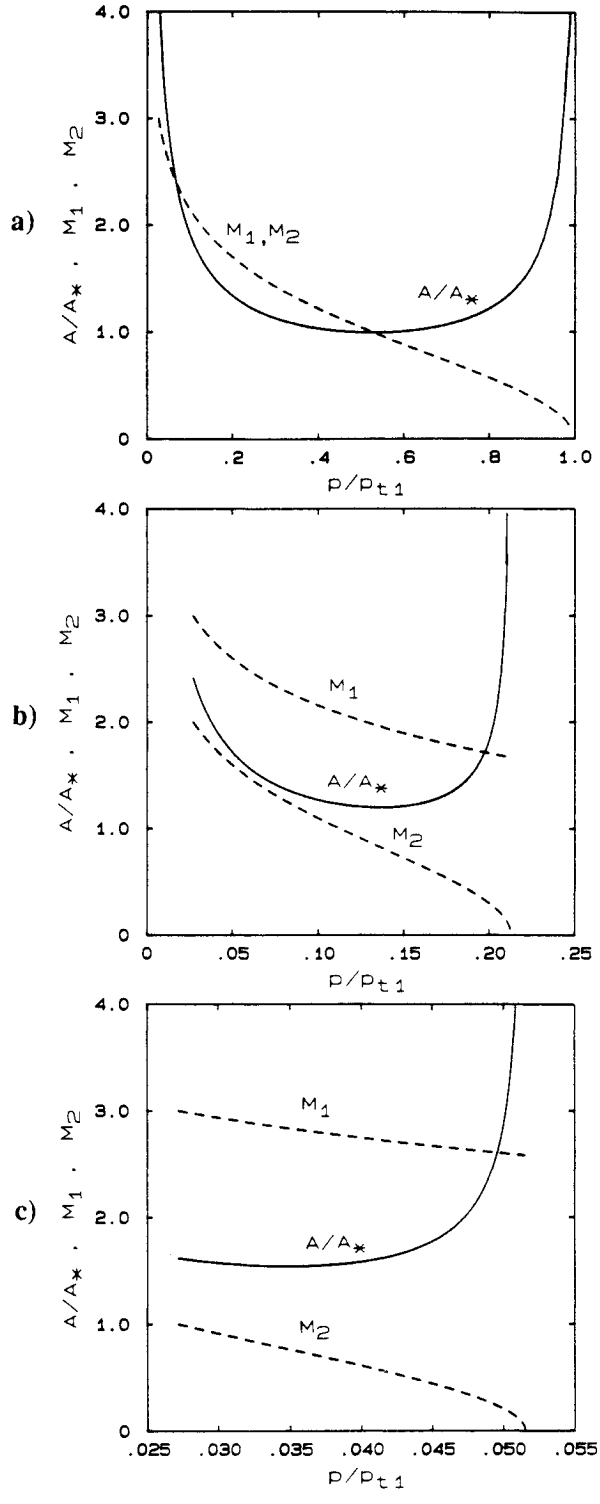

Fig. 2 Diffuser area and Mach numbers vs streamwise static pressure for $\gamma_1 = \gamma_2 = 1.4$ and $A_{2,\infty}/A_{1,\infty} = 1.0$: a) $M_{1,\infty} = M_{2,\infty} = 3.0$; b) $M_{1,\infty} = 3.0$, $M_{2,\infty} = 2.0$; c) $M_{1,\infty} = 3.0$, $M_{2,\infty} = 1.0$.

til the Mach number becomes sonic, at which point A reaches its minimum, $A_{\min}$. In this case, of course, $A_{\min} = A_*$. As $\bar{p}$ increases further, the area increases and the Mach number deceases. Eventually, the Mach number reaches zero as the area becomes infinite. As seen on the figure, pressure recovery is full, i.e., $\bar{p}$ reaches 1 for this uniform case.

In Figure 2b, $M_{1,\infty} = 3$ and $M_{2,\infty} = 2$. The point at which $A_{\min}$ occurs corresponds exactly to the choking condition [Eq. (4)]: M_1 is supersonic and M_2 is subsonic. Notice now that $A_{\min} > A_*$. With further pressure increase, A increases to infinite, M_2 decreases to zero, and M_1 decreases but remains

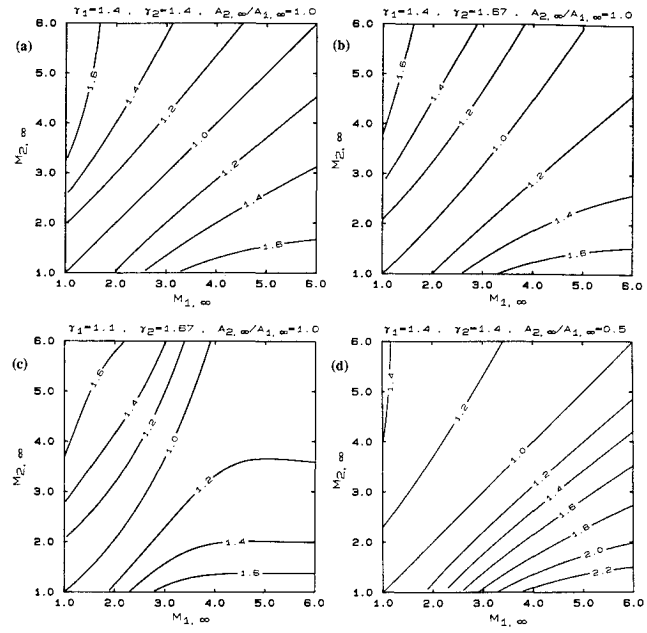

Fig. 3 Contours of constant $A_{\min}/A^*$ vs $M_{1,\infty}$ and $M_{2,\infty}$: a) $\gamma_1 = \gamma_2 = 1.4$, $A_{2,\infty}/A_{1,\infty} = 1.0$; b) $\gamma_1 = 1.4$ $\gamma_2 = 1.67$, $A_{2,\infty}/A_{1,\infty} = 1.0$; c) $\gamma_1 = 1.1$ $\gamma_2 = 1.67$, $A_{2,\infty}/A_{1,\infty} = 1.0$; d) $\gamma_1 = 1.4$ $\gamma_2 = 1.4$, $A_{2,\infty}/A_{1,\infty} = 0.5$.

supersonic. The pressure cannot increase beyond the value where $M_2 = 0$ or the upstream conditions in that stream will break down. Thus, the upper limit for p is $p = p_{t_2}$, with p_{t_2} the lower of the two total pressures. This is the best possible pressure recovery for this model.

While discussing Fig. 2b, it is informative to see how the individual areas A_1 and A_2 change with increasing p. As shown schematically on Fig. 1, A_2 reaches its minimum *before* A reaches $A_{\min}$. At $A = A_{\min}$, A_2 is diverging and M_2 is subsonic, while A_1 is converging and M_1 is supersonic. At $p = p_{t_2}$, A_2 is infinite, but A_1 is finite and still converges. This diffuser design represents the conditions for best pressure recovery.

Figure 2c depicts an extreme case with $M_{1,\infty} = 3$ and $M_{2,\infty} = 1$. The trends are similar to those of Fig. 2b. Notice, however, the large value of $A_{\min}/A_*$ and the small choking margin for this flow: $A_{\min}$ is reached after reducing the area only a few percent.

Of great importance to the tunnel designer and operator is a parametric evaluation of $A_{\min}/A_*$ vs the test section conditions and geometry. From Eq. (11), we have

$$\frac{A_{\min}}{A_*} = f\left(\gamma_1, \gamma_2, M_{1,\infty}, M_{2,\infty}, \frac{A_{2,\infty}}{A_{1,\infty}}\right) \tag{12}$$

In Figs. 3a-3c, contours of equal $A_{\min}/A_*$ are plotted vs $M_{1,\infty}$ and $M_{2,\infty}$ for $A_{2,\infty}/A_{1,\infty} = 1$ and three $\gamma_1 - \gamma_2$ combinations. In Fig. 3d, $\gamma_1 = \gamma_2 = 1.4$, but $A_{2,\infty}/A_{1,\infty} = 0.5$. It is seen that variations in γ have a rather small effect on the second throat area. On the other hand, the area ratio $A_{2,\infty}/A_{1,\infty}$ has a more pronounced effect.

Discussion

The above calculations reflect idealized conditions under which the shear-layer and boundary-layer growth rates are taken to be zero. Clearly, such a model would yield rather optimistic results for the actual wind-tunnel performance. Yet, even under these simplifying assumptions, it is found that the performance of two-stream supersonic wind tunnels is very different from that of one-stream ones, especially when the Mach number difference is large. Choking criteria can be quite severe, as shown on Fig. 3. The requirement that the diffuser exhaust pressure not exceeed the lower of the two total pressures can drastically decrease pressure recovery, as shown on Figs. 2b and 2c.

In an actual tunnel, the finite thickness of the shear layer and of the wall boundary layers will make the situation even worse. Shear layers between two supersonic streams are known to have *positive* displacement thickness.[4] That, combined with the displacement thickness of the boundary layers will decrease the effective diffuser area. On the other hand, the present zero-growth assumption for the shear layer is not bad for a relatively short test section length, because supersonic shear layers grow extremely slowly compared to subsonic ones.[5] Obviously, the longer the channel, the more severe the viscous effects will be. Dutton et al.[6] found that if the channel length of a supersonic-supersonic ejector is very long, the flow inside the ejector may suffer a normal-shock-like deceleration, with an accompanying total pressure loss, static pressure rise, and Mach number decrease to subsonic values.

The second throat areas depicted on Fig. 3 correspond to steady-state, running conditions. They do not reflect the requirements for starting the tunnel. In one-stream tunnels, the minimum second throat area required for starting is considerably larger than that required for running, even under inviscid conditions. It is safe to assume that the same is true for two-stream tunnels, although their starting process is too complex to be addressed here. For $M_{1,\infty}$ and $M_{2,\infty}$ substantially different, the second throat provides minute pressure recovery (Figs. 2b and 2c) and introduces the risk of not being able to start. In that case, it appears best to eliminate the second throat. If, however, pressure recovery turns out to be important, a variable-area diffuser then should be employed.

Acknowledgments

This work has been supported by a research grant from the Rockwell International Foundation Corporation Trust and Contract N00014-85-K-0646 of the U.S. Navy Office of Naval Research.

References

[1]Ferri, A. and Edelman, R., "Some Observations on Heterogeneous Mixing Inside Channels," New York University, New York, Rept. NYU-AA-67-109, Aug. 1967.

[2]Bernstein, A., Heiser, W. H., and Hevenor, C., "Compound-Compressible Nozzle Flow," *Transactions of the ASME,* Vol. 34, Sept. 1967, pp. 548–554.

[3]Cosner, R. R., "Experiments on Thin Airfoils Spanning a Transonic Shear Flow," Ph.D. Thesis, California Institute of Technology, Pasadena, CA, June 1976.

[4]Papamoschou, D., "Experimental Investigation of Heterogeneous Compressible Shear Layers," Ph.D. Thesis, California Institute of Technology, Pasadena, CA, Dec. 1986.

[5]Papamoschou, D. and Roshko, A., "Observations of Supersonic Shear Layers," AIAA Paper 86-0162, Jan. 1986.

[6]Dutton, J C., Mikkelsen, C. D., and Addy, A. L., "A Theoretical and Experimental Investigation of the Constant-Area, Supersonic-Supersonic Ejector," *AIAA Journal,* Vol. 20, Oct. 1982, pp. 1392–1400.

Velocity Profile Model for Two-Dimensional Zero-Pressure Gradient Transitional Boundary Layers

H. Pfeil* and T. Müller†
Technische Hochschule Darmstadt, Darmstadt, Federal Republic of Germany

Received Jan. 8, 1988; revision received Aug. 15, 1988.

*Professor, Institute for Thermal Turbomachines.
†Research Engineer, Institute for Thermal Turbomachines.

Nomenclature

$A_{1,2,3,4}$ = constants of the law of the wall, Eq. (8)
C_T = universal additive constant of the logarithmic law of the wall, = 5
$C_1, \tilde{c}$ = constants of the law of the wall, Eq. (8)
C_{0T} = universal additive constant, Eq. (5)
f = function
H = shape parameter, $= \delta_1/\delta_2$
K = constant, Eq. (13)
m = exponent of Falkner Skan similarity solutions
Re_δ = Reynolds number based on boundary-layer thickness, $= U_\infty \delta/\nu$
Re_1 = Reynolds number based on displacement thickness, $= U_\infty \delta_1/\nu$
Re_2 = Reynolds number based on momentum thickness, $= U_\infty \delta_2/\nu$
Tu = freestream turbulence intensity, $= (\overline{u'^2}/U_0^2)^{0.5}$
u = mean velocity component parallel to the wall
u_{1m} = scaling velocity of the wake function
u_τ = friction velocity, $(\tau_w/\rho)^{0.5}$
u^+ = nondimensional mean velocity, $= u/u_\tau$
U_0 = freestream velocity
U_∞ = freestream velocity at the edge of the boundary layer
X = nondimensional characteristic quantity, $= |y^+ \kappa|_\delta = Re_\delta \omega \kappa$
y = local coordinate normal to the wall
y^+ = nondimensional wall distance, $= y u_\tau/\nu$
β = constant, here $\beta = \frac{3}{4}\pi^2$
δ = boundary-layer thickness
δ_1 = displacement thickness
δ_2 = momentum thickness
η = nondimensional wall distance, $= y/\delta$
κ = constant of the law of the wall, Eq. (8)
κ_T = von Kármán constant, = 0.41
Λ = nondimensional pressure gradient, $= (\delta^2/\nu)(dU_\infty/dx)$
ν = kinematic viscosity
ρ = fluid density
ω = nondimensional friction velocity, $= u_\tau/U_\infty$
Φ_1 = wake function
Φ_2 = law of the wall function
Φ_3 = correction function
τ_w = wall shear stress, $= \rho u_\tau^2$

Indices

a = outer region
i = inner region
I = instability point
L = laminar
P = Pohlhausen
Tr = transition point
T = turbulent
$T1$ = first turbulence profile after transition

I. Introduction

MEASURED turbulent boundary-layer profiles in a plane flow can be described with good agreement by the Coles profile model,[1] especially if the abrupt change in the slope at the outer edge of the boundary layer is eliminated, so that the velocity gradient $\partial u/\partial y|_\delta$ becomes zero.

$$\frac{u_T}{U_\infty} = 1 - \frac{\omega}{\kappa}[\Phi_2(\eta) - \Phi_3(\eta)] - \frac{u_{1m}}{U_\infty}\Phi_1(\eta)$$

$$= 1 - \frac{\omega}{\kappa}[-\ln(\eta) - (\tfrac{1}{2} - 3\eta^4 + 4\eta^5 - 1.5\eta^6)]$$

$$- \frac{u_{1m}}{U_\infty}\cos^2\left(\frac{\pi}{2}\eta\right) \qquad (1)$$